Environ. Sci. Technol. **2003**, *37,* 4855−4863

Distribution of Polycyclic Aromatic Hydrocarbons in the Coastal Region off Macao, China: Assessment of Input Sources and Transport Pathways Using Compositional Analysis

BIXIAN MAI,*,† SHIHUA QI,† EDDY Y. ZENG,‡ QINGSHU YANG,†,§ GAN ZHANG,† JIAMO FU,† GUOYING SHENG,† PINGAN PENG,† AND ZHISHI WANG||

State Key Laboratory of Organic Geochemistry, Guangzhou Institute of Geochemistry, Chinese Academy of Sciences, Guangzhou, 510640, China, Southern California Coastal Water Research Project, 7171 Fenwick Lane, Westminster, California 92683, Institute of Estuarine and Coastal Research, Zhongshan University, Guangzhou, 510275, China, and Faculty of Science and Technology, University of Macao, Macao Special Administrative District, China

The coastal region off Macao is a known depositional zone for persistent organic pollutants (POPs) in the Pearl River Delta and Estuary of southern China and an important gateway for the regional contributions of contamination to the globe. This paper presents a comprehensive assessment of the input sources and transport pathways of polycyclic aromatic hydrocarbons (PAHs) found in the coastal sediments of Macao, based on measurements of 48 2−7 ring PAHs and 7 sulfur/oxygenated (S/O) PAH derivatives in 45 sediment, 13 street dust, and 68 aerosol samples. Total sediment PAHs concentrations ranged from 294 to 12 741 ng/g, categorized as moderate contamination compared to other regions of Asia and the world. In addition, the PAH compounds appeared to be bound more strongly to aromatics-rich soot particles than to natural organic matter, implying a prevailing atmospheric transport route for PAHs to Macao's coast. Compositional analysis and principal component analysis (PCA) suggested that different classes of PAHs in the coastal sediments of Macao may have been derived from different input sources via various transport pathways. For example, alkylated and S/O PAHs were likely derived from fossil fuel leakage and transported to sediments by both aerosols particles and street runoff. High-molecular-weight parent PAHs were predominantly originated from automobile exhausts and distributed by direct and indirect atmospheric deposition. Low-molecular-weight parent PAHs, on the other hand, may have stemmed from lower temperature combustion and fossil fuel (such as diesel) spillage from ships and boats and were transported to sediments by river runoff or direct discharge as well as by air−water exchange.

* Corresponding author phone: 86-20-85290179; fax: 86-20-85290706; e-mail: nancymai@gig.ac.cn.
† Guangzhou Institute of Geochemistry.
‡ Southern California Coastal Water Research Project.
§ Zhongshan University.
|| University of Macao.

Introduction

In recent years scientists have become increasingly concerned about the distribution and fate of POPs in the tropical and subtropical regions of Asia (*1*−*4*), because the tropical mild to high temperatures and heavy rainfalls are able to rapidly dissipate POPs into the atmosphere and aquatic systems from points of usage or discharge. The "global distillation/fractionation" hypothesis (*5*, *6*) suggests that semivolatile and persistent organic compounds may be distilled or fractionated by differential temperatures around the globe. As a result, these chemicals tend to redistribute from tropical point sources to high-latitude areas via single-hop pathway (*6*) or multihop pathway (*5*) based on their volatility and ambient temperatures (*7*). The role of oceans in dictating the global transport and fate of POPs was also addressed (*8*).

The widespread distribution of sedimentary PAHs, an important class of POPs and culprits of carcinogenicity and mutagenicity, has been well documented in industrialized countries, and a vast number of publications are available in the literature. By contrast, only limited sedimentary PAH data have been acquired in recent years from a small range of tropical/subtropical regions in Asia, mostly in southern China (*3*, *9*−*18*). Because most tropical/subtropical regions in Asia are highly populated and generally under rapid economic development and urbanization, a large amount of PAHs generated in these regions may potentially move into other relatively colder regions and therefore contribute significantly to the global pollution problem.

Macao is located at the southern end of the Pearl River Delta, a tropical/subtropical region (21°50′-23°25′N/112°33′-114°10′E) in southern China (Figure 1a). The Delta is subject to typical Asian monsoon climates, i.e., hot and humid in summer with strong southeastern monsoon breezes from the South China Sea, mild with frequent but light rainfalls in spring, and relatively cool and dry in autumn and winter influenced by northeastern monsoon winds from northern China. Average ambient temperature ranges from 19 to 28 °C all year around and an annual volume of rainfall ranges from 1300 to 2280 mm (*19*). The coastal areas off Macao, to some degree, serve as a trap for fluvial suspended particles from the western part of the delta water network (mainly Xijiang River) through one of the major outlets, Modaomen (Figure 1b,c). Suspended solids (especially fine particles) from the eastern and northern parts of the delta water network (Zhujiang, Beijiang, and Dongjiang Rivers) discharged through four other major outlets (Humen, Jiaomen, Honqilimen, and Hengmen) may deposit in Macao's coastal region. Local sources such as municipal sewage disposal, industrial and agricultural discharge, and urban runoff also impact the coastal environment.

A recent sampling of surface and core sediments from 17 locations around the Pearl River Delta indicated that the sediment samples from Macao Harbor had the highest concentrations of chlorinated pesticides, polychlorinated biphenyls, and PAHs (*4*, *16*, *18*, *20*). However, that survey collected and analyzed only three samples from the coast of Macao, and the data were insufficient to evaluate contaminant distribution patterns, input sources, and transport pathways.

The objectives of the present study were to (1) examine the distribution of sediment PAHs in the coast of Macao; (2)

10.1021/es034514k CCC: $25.00
Published on Web 09/25/2003

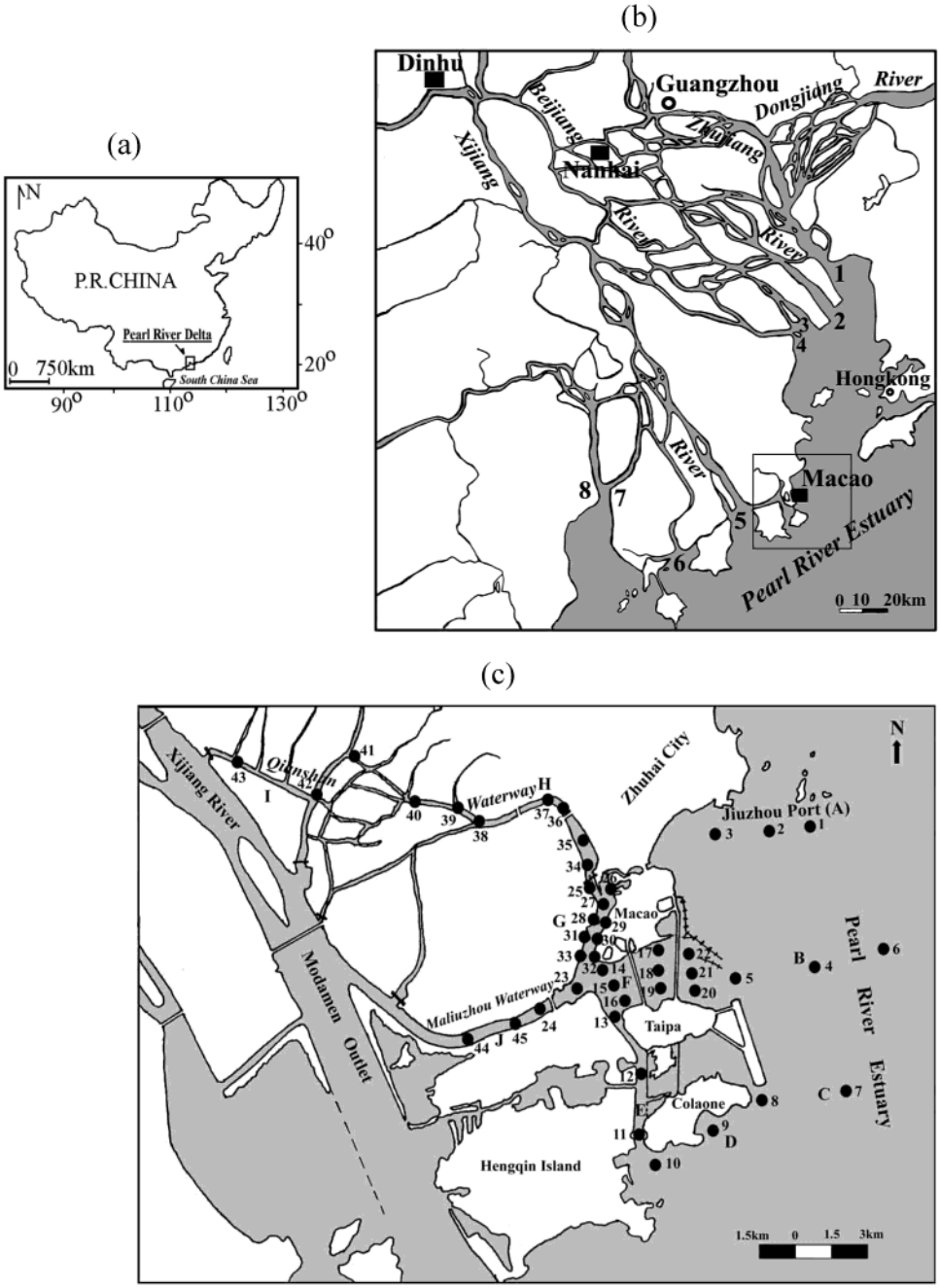

FIGURE 1. (a) Schematic showing the geographical locality of the Pearl River Delta in China. (b) Map of the general study area and aerosol sampling sites (■) around the Pearl River Delta and Estuary with the numbers 1−8 indicating the eight major runoff outlets: 1 − Humen; 2 − Jiaomen; 3 − Honqilimen; 4 − Hengmen; 5 − Modaomen; 6 − Jitimen; 7 − Hutiaomen; and 8 − Yamen. (c) Sediment sampling locations around the coast of Macao: A − Jiuzhou Port; B − Port Exterior; C − East of Colaone Island; D − Southeast of Colaone Island; E − Shizhimen Waterway; F − Nam Van Estuary; G − Port Interior; H − lower Qianshan Waterway; I − upper Qianshan Waterway; and J − Maliuzhou Waterway.

elucidate potential input sources of PAHs; and (3) assess the transport pathways for PAHs to reach the region. To accomplish these objectives, we collected and analyzed sediments from the coastal areas off Macao, street dusts within the city of Macao, and aerosols around Macao and adjacent areas in the Pearl River Delta. PAH compositional indices and principal component analysis (PCA) were employed for data assessment. Sediment PAH data from a previous study (*18*) were also included for comparison.

Experimental Section

Study Site. The coast of Macao locates at the western side of the Pearl River Estuary (Figure 1b), one of the largest estuaries in the world, covering an area of ~2100 km^2 and connecting the continent with the South China Sea. Each year approximately 3.26×10^{11} m^3 of freshwater containing 7.07×10^8 tons of suspended particles flow into the estuary via eight major outlets (*21*). Within the estuary, a southwestward coastal current (called the South China coastal current), originating from the counterclockwise Corelis force in the Northern Hemisphere and the prevailing westward wind in the region, tends to transport freshly discharged materials from north and east to southwest (*21*). The southwest part of the estuary is characterized by high saline gradients and dissipative energy, which allows coagulation and deposition of fluvial fine suspended particles. As a

comparison, the sedimentation rate in the west coast of the estuary is 1.52−3.85 cm/yr, higher than that (0.86 cm/yr) in the east coast (*4*).

Aerosol samples were collected from three locations representing three levels of anthropogenic pollution around the Pearl River Delta (Figure 1b). In addition to a sampling site in Macao representing the direct atmospheric input source to the coast of Macao, two other sites were also chosen for sampling. The first site was in the City of Nanhai, located at the center of the delta and representative of mid-level of anthropogenic pollution in the region. The second site was on the Dinhu Mountain at the west side of the delta and adjacent to Xijiang River. This location was chosen as a background reference of atmospheric pollution, because atmospheric particles carried by prevailing westward winds are blocked by a cluster of mountains and hills in the west of the delta.

Sample Collection. Forty-five sediment samples were collected around the coast of Macao (Figure 1c) between October 14 and 17, 1999, using a stainless steel grab sampler. The sampling stations were selected as such to cover the entire coastal region with various urban, suburban, rural, and estuarine areas. Top 20-cm sediments were scooped using a precleaned stainless steel scoop into solvent-rinsed aluminum jars. A previous study obtained the sediment accumulation rate of 1.87 cm/year for a sediment core (ZJ-9) in Nam Van Estuary (*4*); hence a 0−20 cm layer of sediments represented approximately 10 years of deposition. Thirteen street dust samples were collected using a straw brush from 13 heavily trafficked streets of Macao Island in November 1998 and were stored in solvent-rinsed tight-sealed amber vials. A number of aerosol samples were collected in 1998 and 1999 from Macao, Nanhai, and Dinhu Mountain using high-volume air samplers described previously (*22*). Sample volumes ranged from 681 to 1584 m^3. Glass-fiber filters containing aerosol particles were wrapped in aluminum foil. All the samples were transported on ice to a laboratory where they were stored at −20 °C until analyzed. Detailed descriptions of the sample characteristics are provided in Table S1 of Supporting Information ("S" designates tables or figures in Supporting Information thereafter).

Chemical Analysis. The analytical procedure used for extraction, separation, and measurement of PAHs in sediment, aerosol, and street dust samples was detailed elsewhere (*18*, *22*), and only a brief description is given here. A mixture of deuterated PAH compounds (naphthalene-d_8, acenaphthene-d_{10}, phenanthrene-d_{10}, chrysene-d_{12}, and perylene-d_{12}) as recovery surrogate standards was added to all the samples prior to extraction. Freeze-dried sediment samples were Soxhlet-extracted with methylene chloride. Street dust and aerosol samples were ultrasonically extracted with methylene chloride in aluminum foil lined amber belchers. The extracts were concentrated, solvent-exchanged to hexane, and purified using a 1:2 alumina:silica column chromatography. The first fraction, containing aliphatic hydrocarbons, was eluted with 15 mL of hexane. The second fraction containing PAHs was collected by eluting 5 mL of hexane and 70 mL of methylene chloride:hexane (30:70). The PAH fraction was concentrated to 0.4 mL under a gentle N_2 stream. A known amount of internal standard (hexamethylbenzene) was added to the extract prior to instrumental analysis.

Concentrations of PAHs, including 30 parent components, 18 alkylated homologues, and 7 S/O PAH derivatives (Tables S2−S4), were determined with a Hewlett-Packard 5890 series gas chromatograph/5972 mass spectrometer in the selective ion monitoring mode, and chromatographic separation was provided by a 50 m × 0.32 mm-i.d. (0.17 μm film thickness) DB-5MS capillary column (J&W Scientific, Folsom, CA). Detailed instrumental conditions were described previously (*18*). Quantitation was done using the internal calibration method (five-point calibration). Final PAH concentrations were corrected from the recoveries of the surrogate standards. Surrogate recoveries were 58 ± 12% for naphthalene-d_8, 75 ± 10% for acenaphthene-d_{10}, 93 ± 8% for phenanthrene-d_{10}, 94 ± 10% for chrysene-d_{12}, and 90 ± 9% for perylene-d_{12} with sediment samples (n = 45) and were 45 ± 25% for naphthalene-d_8, 65 ± 23% for acenaphthene-d_{10}, 91 ± 18% for phenanthrene-d_{10}, 92 ± 19% for chrysene-d_{12}, and 89 ± 17% for perylene-d_{12} with aerosol and dust samples (n = 81).

For each batch of 20 field samples, a procedural blank (solvent with a clean GF/F filter), a spiked blank (16 PAH standards spiked into solvent with a clean GF/F filter), a matrix spiked sample (16 PAH standards spiked into pre-extracted sediment, dust or aerosol), a matrix spiked duplicate, a sample duplicate (only for sediment and dust samples), and a National Institute of Standards and Technology (NIST; Gaithersburg, MD) 1941 reference sample were processed. Field blank (clean GF/F filters exposed to air during aerosol sampling) and procedural blank samples contained no detectable amounts of the target analytes except that naphthalene was detected in the field blanks; hence, data were blank corrected. The relative percent difference for individual PAHs identified in paired duplicate samples (n = 4) was all < 15%. Recoveries of all the PAHs in the NIST 1941 sample were between 80 and 120% of the certified values. Nominal detection limits for individual PAH compounds ranged from 0.2 to 2 ng/g (dry wt) for 10 g of sediment, 2−20 ng/g (dry wt) for 1 g of street dust, and 0.008−0.08 ng/m^3 for 500 m^3 of aerosol, respectively. Actual reporting limits were adjusted based on the sample sizes used.

Measurements of Sediment Organic Carbon and Black Carbon. Five grams of freeze-dried sediment was treated with 10% HCl solution to remove inorganic carbon and dried overnight at 60 °C. An aliquot of the sample was used to determine organic carbon (OC) and total nitrogen (TN) concentrations. Soot carbon content was measured by a modified method of Gustafsson et al. (*23*). Subsamples upon acidification were further oxidized thermally in a muffle furnace at 375 °C for 24 h under oxygen-saturated air. The samples were reweighed after cooling in a desiccator for mass balance calculation and then used for black carbon (BC) determination. OC, TN, and BC were quantified with a CHN-O RAPID elemental analyzer (Heraus, Germany). Acetanilide was used as external standard (instrument detection limit = 10 ± 0.2 μg/g for carbon). All values were normalized to the initial mass of the sample prior to any treatment.

Measurements of Sediment Minerals. X-ray diffraction techniques were used to measure the concentrations of quartz, plagioclase, kaolinite, illite, montmorillonite, and chlorite in the sediment samples. Only total clay mineral contents (sum of kaolinite, illite, montmorillonite, and chlorite) are reported here.

Data Analysis. Data analysis included calculating individual and total PAH concentrations, summarizing PAH compositional indices or ratios, correlating various concentration and composition related parameters, and performing PCA. Two total PAH concentrations were calculated. The first one (tPAH1) was the sum of the concentrations of all PAH compounds (Table S2) except for perylene. The second one (tPAH2) was the sum of the concentrations of phenanthrene, anthracene, methylphenanthrenes (1-,2-,3-, and 9-methylphenanthrenes), fluoranthene, pyrene, benzo[*a*]anthracene, chrysene, benzo[*b*+*k*]fluoranthenes, benzo[*e*]pyrene, benzo[*a*]pyrene, indeno[1,2,3-*cd*]pyrene, and benzo[*g*,*h*,*i*]perylene and was used for comparison with a previous study (*3*).

The PAH compositional indices or ratios used in the assessment included alkylated PAHs/parent PAHs (A-PAHs/P-PAHs) (excluding perylene), low- molecular-weight parent

PAHs (phenanthrene to pyrene)/high-molecular-weight parent PAHs (benzo[*a*]anthracene to coronene except perylene) (LMW-PAHs/HMW-PAHs), methylphenanthrenes/phenanthrene (MP/P), fluoranthene/pyrene (Fl/Py), benzo[*a*]anthracene/chrysene (B*a*A/Chr), benzo[*a*]pyrene/benzo[*e*]pyrene (B*b*P/B*e*P), indeno[1,2,3-*cd*]pyrene/benzo[*g,h,i*]perylene (InP/B*ghi*P), and benzo[*b*]fluoranthene/benzo[*k*]fluoranthene (B*b*F/B*k*F).

Finally, PCA was used to explore the similarities or differences among the samples with complex compositional information and facilitate the assessment of input sources and transport pathways. Prior to analysis, nondetectable values were replaced with random numbers between zero and the sample-dependent reporting limits. This ensured the analysis was not influenced by spurious correlations between compounds that were not detected in some samples. All 55 PAH components or homologues in sediment and street dust samples (Tables S2 and S3) were submitted to PCA, whereas naphthalene, biphenyl, acenaphthylene, acenaphthene, and fluorene as well as their alkylated homologues were removed from the aerosol data before PCA as their concentrations were below reporting limits in a number of aerosol samples (Table S4). PCA with varimax rotation was performed using the software package STATISTICA (SYSTAT 5.0). Only the principal components with eigenvalues > 0.9 were retained, and only the principal component loadings with absolute values greater than 0.20, accounting for >2% of the variance in a given variable, were considered. Although normalization and fractionalization have been suggested as to minimize the differences between samples in terms of absolute PAH concentrations (*24*−*26*), they did not yield better interpretation of our data probably because of the small range of the PAH concentrations.

Results and Discussion

Distribution of Sediment PAHs. The concentrations of total PAHs (tPAH1) in sediments ranged from 294 to 12 741 ng/g (Table 1). Spatially, sediments collected from Port Interior near Macao Island had the highest PAH concentrations, while two rural waterways (upper Qianshan and Maliuzhou) were the least contaminated by PAHs. It is interesting to note that sediments collected offshore (Jiuzhou Port, Port Exterior, and East of Colaone Island) contained comparable amounts of PAHs as those from most of the inshore locations (e.g., Southeast of Colaone Island, Shizhimen Waterway, Nam Van Estuary, and lower Qianshan Waterway). The concentrations of total parent PAHs (tPAH2) also followed the similar distribution pattern as those of tPAH1, and the ratios of tPAH2/tPAH1 were 0.30 ± 0.06 (n = 45) for all the samples.

A comparison of the magnitude of PAH contamination in the coast of Macao with those in other parts of the Pearl River Delta, Asia, and the globe was made to provide a large perspective. In this comparison, values of tPAH2 were utilized as they were also measured in other comparable studies (*3*, *18*). The magnitude of PAH contamination in the coast of Macao (80−8415 ng/g) was slightly lower than that (451−11 148 ng/g) in the Zhujiang River (Figure 2) that has been regarded as the most contaminated river stream in the Pearl River Delta but was comparable to other areas of the Pearl River Delta (e.g., Xijiang River and Pearl River Estuary). In general, PAH concentrations in sediments of Macao's coastal region and the rest of the Pearl River Delta were lower than or comparable to those in Tokyo Bay (534−292 370 ng/g), higher than those in riverine and coastal sediments of Malaysia (4−924 ng/g), and well around the midpoint of the global PAH concentration range (*3*).

Concentrations of perylene accounted for 9−75% of total parent PAHs (including perylene) (Table 1), with the highest concentrations mostly occurring at the rural sites (e.g., Qianshan Waterway). A linear regression analysis yielded a poor correlation (r^2 = 0.05−0.18) between the concentrations of perylene and the 5−6 ring parent PAH compounds (e.g.,

TABLE 1. Concentrations of Organic Carbon (OC), Black Carbon (BC), Clays, Total PAHs, and Perylene in Coastal Sediments off Macao

sample[a]	OC (mg/g)	BC (mg/g)	clay[b] (g/g)	tPAH1[c] (ng/g)	tPAH2[d] (ng/g)	perylene (ng/g)
A. Jiuzhou Port (Estuarine, Offshore)						
MC01	11.9	1.16	0.65	1588	444	165
MC02	11.5	1.17	nm[e]	1566	462	149
MC03	11.0	1.28	0.69	1624	391	116
B. Port Exterior (Estuarine, Offshore)						
MC04	11.4	1.13	0.62	1424	398	66
MC05	15.1	1.67	0.47	2536	779	183
MC06	12.2	1.47	0.69	2043	534	127
C. East of Colaone Island (Estuarine, Offshore)						
MC07	11.2	1.18	0.69	1662	433	116
D. Southeast of Colaone Island (Suburban, Inshore)						
MC08	9.8	0.58	0.54	717	217	141
MC09	13.4	1.30	0.51	2057	675	250
MC10	15.5	1.39	0.70	2019	605	207
E. Shizhimen Waterway (Suburban, Inshore)						
MC11	16.0	1.72	0.67	2610	865	293
MC12	10.6	1.29	0.19	1762	493	135
MC13	10.5	1.31	0.63	1597	402	235
F. Nam Van Estuary (Estuarine, Inshore)						
MC14	11.9	1.29	nm[e]	1842	481	451
MC15	6.6	0.79	0.40	993	244	82
MC16	13.1	1.49	0.61	2482	737	282
MC17	11.1	1.36	0.52	2494	723	307
MC18	6.1	1.05	0.25	722	218	80
MC19	7.8	1.13	0.40	1910	529	99
MC20	12.2	1.60	0.43	2261	723	312
MC21	10.5	1.52	0.47	2183	608	251
MC22	11.9	1.22	0.67	1656	589	220
G. Port Interior (Urban, Inshore)						
MC25	11.5	0.98	0.28	4099	1570	176
MC26	17.0	1.44	0.62	5864	1145	288
MC27	4.2	0.60	0.39	4017	2231	109
MC28	15.9	1.36	0.50	6719	1839	358
MC29	14.4	2.00	0.45	4350	1138	427
MC30	15.8	1.72	0.62	5133	1049	303
MC31	15.1	1.95	0.60	4774	964	402
MC32	13.6	1.44	0.71	12741	8415	289
MC33	14.7	1.87	0.50	7948	3873	420
H. Lower Qianshan Waterway (Rural, Inshore)						
MC34	9.5	1.53	0.37	2048	518	271
MC35	15.7	1.81	0.42	2560	640	446
MC36	14.2	2.10	0.64	3025	1004	348
MC37	12.7	1.51	0.49	2334	664	261
MC38	12.1	1.31	0.48	1845	517	238
I. Upper Qianshan Waterway (Rural, Inshore)						
MC39	13.5	1.33	0.48	1867	548	472
MC40	12.9	1.43	0.49	1530	571	427
MC41	10.3	0.66	0.40	717	252	398
MC42	13.8	1.89	0.53	2534	841	668
MC43	8.7	0.62	0.43	695	232	709
J. Maliuzhou Waterway (Rural, Inshore)						
MC23	9.5	0.78	0.56	411	148	76
MC24	8.9	0.56	0.52	294	80	58
MC44	8.5	1.37	0.48	1829	647	152
MC45	12.2	1.38	0.60	1989	580	175

[a] Sampling stations are depicted in Figure 1c but labeled with alphabetic numbers only. [b] Clay = sum of kaolinite, illite, montmorillonite, and chlorite. [c] tPAH1 = sum of the concentrations of all PAH components (Table 2 of Supporting Information) except for perylene. [d] tPAH2 = sum of the concentrations of phenanthrene, anthracene, methylphenanthrenes (1-,2-,3-, and 9-methylphenanthrenes), fluoranthene, pyrene, benzo[*a*]anthracene, chrysene, benzo[*b*+*k*]fluoranthenes, benzo[*e*]pyrene, benzo[*a*]pyrene, indeno[1,2,3-*cd*]pyrene, and benzo[*g,h,i*]perylene. [e] Not measured.

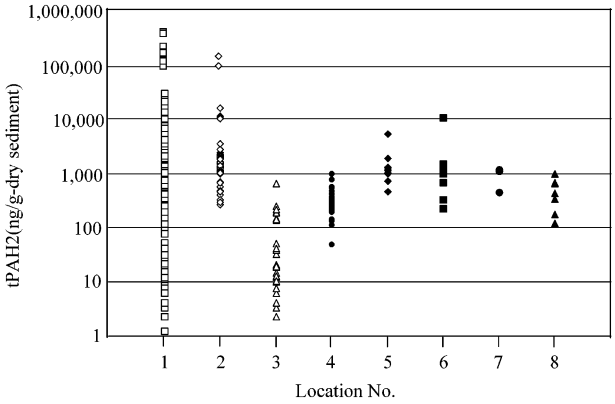

FIGURE 2. Concentrations of total parent PAHs (tPAH2; see text for detailed explanation) in sediments of Macao and the Pearl River Delta in comparison with those in Malaysian, Tokyo, and global sediments (*3*). Location numbers represent sediments collected from the following: 1 − Globe; 2 − Tokyo; 3 − Malaysia; 4 − coast of Macao (except for Port Interior); 5 − Port Interior; 6 − Zhujiang River; 7 − Xijiang River; and 8 − Pearl River Estuary.

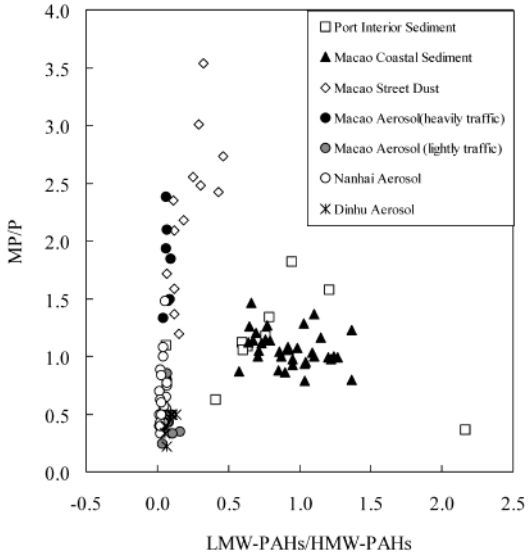

FIGURE 3. Values of methylphenanthrenes/phenanthrene (MP/P) and low-molecular-weight parent PAHs/high-molecular-weight parent PAHs (LMW-PAHs/HMW-PAHs) determined in sediment, aerosol, and street dust samples from the coast of Macao and the Pearl River Delta. Sampling locations are shown in Figure 1.

benzo[*b*]fluoranthene, benzo[*k*]fluoranthene, benzo[*e*]pyrene, benzo[*a*]pyrene, indeno[1,2,3-*cd*]pyrene, dibenzo[*a,h*]anthracene, and benzo[*g,h,i*]perylene). These parent PAH compounds are believed to originate from anthropogenic combustion/pyrogenic sources, and their concentrations were well correlated with each other ($r^2 > 0.9$) in all the sediment samples. This was consistent with several previous studies that attributed predominant perylene concentrations in freshwater sediment (*27*−*30*) and marine sediments (*31*, *32*) to natural diagenetic processes of biogenic precursors (e.g., perylenequinone pigments). On the other hand, retene has also been attributed to natural source inputs (e.g., dehydrogenation and aromatization of abietie acid, a diterpenoid during diagenesis) (*27*, *33*), but its concentrations were significantly ($r^2 > 0.60$) correlated with other alkylated PAH compounds in the present study (with retene accounting for 0.7−3.0% of total alkylated PAHs). In addition, the presence of abundant retene in aquatic environments has been suggested as an indicator of anthropogenic inputs, such as effluents from paper milling processes (*34*), and used as a molecular marker of wood combustion in ambient air (*35*). This assessment suggests that retene may have been derived from anthropogenic sources rather than diagenetic processes in our study site. For this reason, perylene was excluded from and retene was included in tPAH1.

Correlation of PAHs with OC, BC, and Clay Contents. A strong correlation ($r^2 = 0.87$) was found between tPAH1 and BC concentrations in all but Port Interior sediments. Conversely, the correlations between tPAH1 and OC concentrations and between tPAH1 and clay contents were moderate ($r^2 = 0.49$;) and poor ($r^2 = 0.04$;), respectively (Figure S1). In addition, poor correlations ($r^2 = 0.0007-0.179$) were found between tPAH1 and BC, OC, and clay contents in the heaviest polluted Port Interior sediments. The preferential association of PAHs with carbonaceous particles (such as carbon soot) in addition to OC has been reported in soils and sediments by other researchers (*36*−*42*). For example, previous investigations observed significant correlations between total PAH concentrations and both BC (*23*, *43*, *44*) and OC concentrations in riverine/coastal systems (*11*, *45*−*47*). In line with these results, our data suggested that the PAHs in the coastal sediments of Macao were more strongly bound to aromatics-rich soot particles than to natural organic matter, implying an important role played by atmospheric transport in distributing PAHs to the coast of Macao.

Evaluation of Sediment PAH Sources (Petrogenic vs Pyrogenic). Combustion processes and release of uncombusted petroleum products are the two main sources of anthropogenic PAHs found in the environment. In general, parent PAHs are largely produced by incomplete combustion of fossil fuels and plant material or natural diagenesis, whereas alkylated homologues mainly originate from petrogenic sources (*48*−*50*). Of combustion-derived PAHs, low-molecular-weight parent PAHs and/or alkylated homologues are abundantly produced at low to moderate temperatures (*48*, *49*), while high-molecular-weight parent PAHs are generated at high temperatures (*51*). It should be noted that petroleum-derived residues also contain relatively high abundances of two- and three-ring PAHs (*33*). These general observations provide useful guidelines for utilizing PAH compositional indices or ratios to apportion the anthropogenic sources of PAH.

The ratios of A-PAHs/P-PAHs and LMW-PAHs/HMW-PAHs in the Port Interior sediments ranged from 0.4 to 3.5 and 0.4 to 2.16, respectively (Figure S2), although the total PAHs (both tPAH1 and tPAH2) concentrations varied in a relatively small range (Table 1). This might reflect the distinctly different PAH input sources to this specific area. The same ratios ranged from 1.04 to 2.40 and 0.6 to 1.4, respectively, in other sediment samples (Figure S2), probably signaling that PAH input sources were similar. As the sampling sites in Port Interior are adjacent to Macao Island (Figure 1c), a highly urbanized district, local discharge may have been the dominant source of PAHs. Nevertheless, the sediment PAHs in the coast of Macao appeared to be of both petrogenic and pyrogenic origins.

The next compositional index examined was MP/P, a widely used indicator to differentiate between petrogenic and pyrogenic sources. A value of MP/P < 1 was generally found in combustion mixtures, whereas residues of unburned fossil fuel typically displayed M/MP values of 2−6 (*3*, *52*, *53*). In the present study, street dust samples exhibited MP/P values of 1.2−3.5 (Figure 3). Previous studies obtained MP/P values of 0.81−4.14 and 0.57−1.80 in street dust samples from Malaysia and Tokyo, Japan, that were presumably influenced by used crankcase oil and derived from automobile exhausts, respectively (*3*, *54*). If the same argument was applicable to our samples, it suggested that street dusts contained PAHs of largely petrogenic origin. However, the PAH profiles in the street dust samples were depleted in

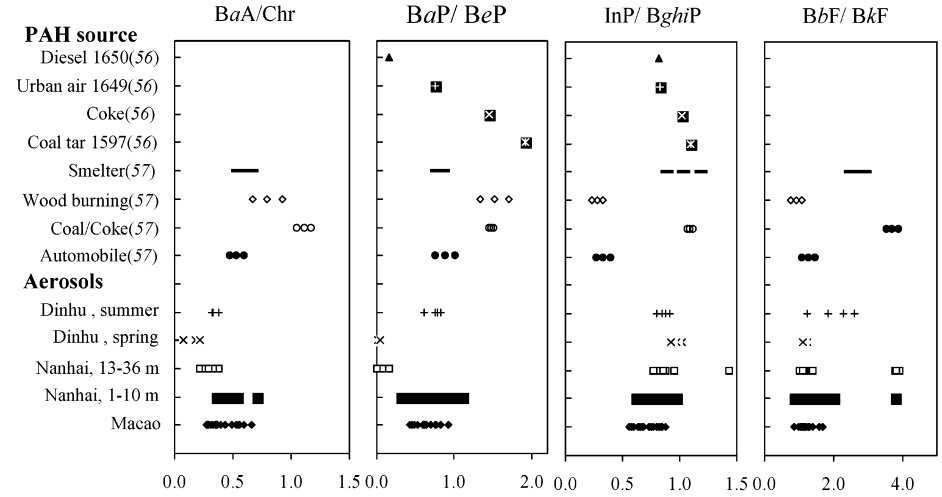

FIGURE 4. Comparison of benzo[*a*]anthracene/chrysene (B*a*A/Chr), benzo[*a*]pyrene/benzo[*e*]pyrene (B*a*P/B*e*P), indeno[1,2,3-*cd*]pyrene/benzo[*g,h,i*]perylene (InP/B*ghi*P), and benzo[*b*]fluoranthene/benzo[*k*]fluoranthene (B*b*F/B*k*F) determined in the aerosol samples from the present study with published data for known PAH sources.

LMW-PAHs (Figure S3c) when compared with those in the Tokyo street dust (e.g., the ratio of Fl+Py/∑COM was 12.7−50.1 in Macao dust samples while it was 37−54 in Tokyo dust samples, where ∑COM was the sum of parent PAHs from fluoranthene to benzo[*g,h,i*]perylene (*54*)) and Malaysia dust samples (*3*). Therefore, the lower LMW-PAHs/HMW-PAHs values (Figure 3) in our street dust samples were indeed indicative of relatively higher degree of high temperature pyrogenic contamination, likely from vehicular exhausts, in Macao street dust than in Tokyo and Malaysia street dust.

Aerosol samples from heavily trafficked streets of Macao exhibited MP/P values of 1.2−3.5, while aerosol samples collected from Dinhu, Nanhai, and lightly trafficked sites of Macao had MP/P values of 0.24−1.0. The low MP/P values and high concentrations of HMW-PAHs (Figures S3e−h) in these aerosol samples probably point to a prevailing pyrogenic source for PAHs in the atmosphere.

The MP/P values (0.63−1.82) in the coastal sediments of Macao were in the mid range of those in all the street dust and aerosol samples (0.24−3.5) (Figure 3), suggesting a combined petrogenic and pyrogenic input source of PAHs to the coastal sediments. The relatively higher LMW-PAHs/HMW-PAHs ratios in sediment samples than in street dust samples (Figures 3 and S3b,c) indicated that PAHs of slightly different sources, i.e., PAHs from low-temperature combustion and petroleum-derived residues, were transported to the coastal sediments as well. In fact, the coast of Macao is a busy waterway that a great number of commercial ships and boats pass by daily to transport merchandise to Macao and the western Pearl River Delta. Exhausts from low-temperature combustion engines as well as accidental fossil fuel spill could have certain impact on the PAH inputs to the coastal sediment. An independent verification of this argument can be achieved from a comparison of the Fl/Py ratios. We obtained Fl/Py values of 0.8−1.16 in our sediment samples, close to the Fl/Py values of 0.9 for fuel oils (*55*) and of 1.10 for a diesel particulate standard, NIST SRM 1649 (*56*). More quantitative assessments on the contributions of PAHs from different sources to Macao coastal sediments will be made with PCA later.

Differentiation of Pyrogenic PAH Sources by Compositional Analysis. A number of combustion sources, such as automobile exhaust, coal/coke combustion, forest fires, household heating stoves, biomass burning, and smelters, may release PAHs to the environment. The isomer ratios of B*a*A/Chr, B*a*P/B*e*P, InP/B*ghi*P, and B*b*F/B*k*F have been proposed as indicators to differentiate between pyrogenic PAH sources, because these PAH isomer pairs have similar thermodynamic partitioning and kinetic mass transfer coefficients and are diluted equally upon advective mixing with natural particulate matter (*34*, *57*). Furthermore, a large portion of combustion-derived PAHs is usually associated with aerosol particles in the atmosphere (*58*).

Aerosol samples collected from Macao and Nanhai at the altitudes of 1−10 m (Figure 4), both characteristic of localized emissions, had similar values for the PAH isomer ratios that from Dinhu Mountain in summer. The PAH isomer ratios in aerosols collected from Nanhai at the altitudes of 13−36 m and Dinhu Mountain in spring were also similar, but these aerosol samples had slightly different B*a*P/B*e*P values compared to other aerosol samples (Figure 4).

The mean B*a*A/Chr (0.42 ± 0.09), B*a*P/B*e*P (0.68 ± 0.20), and B*b*F/B*k*F (1.33 ± 0.48) values in the aerosol samples were comparable to those in the automobile combustion source samples (0.53 ± 0.06, 0.88 ± 0.13, and 1.26 ± 0.19, respectively) (*57*) and SRM 1649 urban air reference standard (0.75 for B*a*P/B*e*P) (*59*). Conversely, the mean InP/B*ghi*P ratio (0.79 ± 0.10) was higher than that in the automobile combustion source samples (0.33 ± 0.06) (*57*) but was similar to those in SRM 1649 urban air particulate (0.83) and SRM 1650 diesel particulate (0.82) (*59*). Colmsjö et al. (*60*) also observed InP/B*ghi*P ratios of less than 1.0 when automotive sources of PAHs dominated. In addition, the PCA results (shown in the next section) indicated that the concentrations of InP and B*ghi*P were correlated with those of B*a*P, B*e*P, B*b*F, and B*k*F in all the aerosol samples. Taken together, the limited compositional analysis suggested that vehicular emission from fossil fuel combustion appeared to be the predominant source of combustion-derived PAHs to the atmosphere of the Pearl River Delta.

Source Apportionment by Principal Component Analysis. **Coastal Sediments.** Five principal components (PC1, PC2, PC3, PC4, and PC5) were identified based on PAH loadings and accounted for 30%, 28%, 18%, 7%, and 2%, respectively, of the total variance (Figure S4). PC1 was mostly associated with alkylated and S/O PAHs and considered a representative of petrogenic sources because of a high degree of alkylation profiles for S/O PAHs and a strongly positive correlation between alkylated PAHs and S/O PAHs. PC2 was dominated by high-molecular-weight parent PAHs and could be attributed to high temperature combustion sources. PC3 was characterized by high loadings of low-molecular-weight parent PAHs, such as fluorene, phenanthrene, anthracene, fluoranthene, and pyrene. PC4 was largely represented by

moderately volatile PAHs (naphthalene, biphenyl, methylnaphthalenes, and dimethylnaphalenes). Finally, PC5 was characterized by a high loading of perylene, thought to originate from diagenetic alteration of terrestrial organic matter (*29*−*34*). Score plot of PC1, PC2, and PC3 (Figure S5), which collectively accounted for 76% of the total variance, grouped all but Port Interior sediments into one cluster that had intermediate values of both PC1 and PC2. This suggested that all PAH inputs were quite evenly distributed in the coastal sediments of Macao except for the Port Interior sediments.

The fact that parent PAHs were clustered into three groups based on their volatility suggested that the different physical-chemical properties of the compounds may have dictated the modes of entry for these compounds. Notably, the most volatile PAH compounds (PC4) could enter the water body via air−water exchange, partition into organic-rich suspended particles, and deposit onto the bottom sediments. This notion is consistent with previous findings implying that gas flux was an important route of delivering PAHs to the water column in areas such as Chesapeake Bay (*47*, *61*), San Francisco Estuary (*62*), and the Great Lakes (*63*−*65*). Our analysis of water column samples collected from the coast of Macao indicated that the concentrations of total PAHs in the dissolved phase (4663−7889 ng/L) were much higher than those in the particulate phase (335−960 ng/L), and the 2−3 ring PAHs comprised more than 95% of the total PAHs (Luo and Mai, unpublished data). These results also agreed with previous assessments that air−water exchange could result in high abundances of low-molecular-weight PAHs in the water body (*65*, *66*).

Street Dust. Eighty percent of the total variance could be explained with the first two principal components, PC1 and PC2 (Figure S6a). PC1, accounting for 57% of the variance, was predominantly comprised of low-molecular-weight (naphthalene to benzo[*a*]anthracene), alkylated, and S/O PAHs and was categorized as being petrogenically originated. PC2, accounting for 23% of the variance, was mainly contributed from high-molecular-weight PAHs (benzo[*b*]-fluoranthene to dibenzopyrenes) and exhibited weak correlation with PC1 ($r^2 = 0.2-0.3$). Perylene contributed high loadings to PC2 and was positively correlated with other pyrolytic PAHs (high-molecular-weight parent PAHs), indicating that perylene found in street dust samples might be of pyrogenic origin. Score plot of PC1 vs PC2 shows no apparent grouping of the samples geographically (Figure S6b). Instead, the PAH composition in street dust samples probably reflected contributions from leakage of crankcase oil (petrogenic) and vehicular exhausts (pyrogenic).

Aerosols. PC1 and PC2 accounted for 89 and 80% of the variances in the Macao and Nanhai aerosol samples, respectively (Figure S7). PC1, describing 49 and 39% of the variances, contained mostly alkylated and S/O PAHs. PC2, responsible for 40 and 41% of the variances, consisted of high-molecular-weight PAHs (benzo[*b*]fluoranthene to dibenzopyrenes) of pyrolytic origins. Among individual parent PAHs, phenanthrene, anthracene, fluoranthene, pyrene, benzo[*g*,*h*,*i*]fluoranthene, and cyclopenta[*cd*]pyrene had moderate loadings for both PC1 and PC2 in Macao aerosols but high loadings for PC1 in Nanhai aerosols except for cyclopenta[*cd*]pyrene which had moderate loadings for both PC1 and PC2. In addition, benzo[*a*]anthracene, chrysene, and triphenylene contributed high loadings to PC1 in Macao aerosols but moderate loadings to both PC1 and PC2 in Nanhai aerosols. These results were probably indicative of both pyrogenic and petrogenic origins for the relatively low-molecular-weight parent PAHs in the aerosols. It is interesting to note that dibenzo[*a*,*c*]anthracene had different PC loadings compared to other high-molecular-weight PAHs in Macao aerosols. Similarly, dibenzofuran and dibenzothiophene contributed different PC loadings to Nanhai aerosols compared to other S/O PAHs. Dibenzothiophene is a tracer to combustion of sulfur-containing fuels such as coal (*56*, *67*), but no specific sources have been identified for dibenzo-[*a*,*c*]anthracene and dibenzofuran.

PC1 and PC2 score plots for Macao and Nanhai aerosols (Figure S8) show that most samples except those from point sources (sample nos. GS 1 to HS-3 and NH34 to NH40 from traffic emission and QT-1 to QT-3 from combustion of asphalt in Table S1) are grouped near the origin, indicating a small variability of PAH compositional patterns among the samples. Macao samples from point sources such as traffic emissions had large contributions to PC1, but those collected near asphalt combustion sources showed high PC2 values. On the other hand, Nanhai samples scattering away from the origin were collected near a major highway and exhibited distinctly different PAH compositions.

Eighty-nine percent of the total variance for Dinhu Mountain aerosols was distributed to PC1 and PC2 (Figure S9a). All analytes except for benzo[*a*]anthracene, triphenylene, benzo[*a*]fluoranthene, benzo[*a*]pyrene, dibenzo[*a*,*c*]-anthracene, and dibenzo[*def*,*mn*]chrysene contributed to PC1 that accounted for 71% of the variance. Such a pattern suggests that PAHs were derived from nonpoint sources (e.g., atmospheric transport from urban and industrial areas). The smaller contributions of the indicated compounds to PC1 relative to PC2 could be attributed to their vulnerability to photodegradation (*68*). Therefore, PC2 signaled the degree of photodegradation as a function of transport distances and modes (long-range transport from north and northeast and short-range transport from southeast). The PC1 and PC2 score plot (Figure S9b) clearly displays the separability of aerosol samples collected in spring and summer, respectively, with respect to PC1 values. The spring samples had higher contributions to PC1 and relatively lower contributions to PC2 than the summer samples, suggesting that the spring samples were enriched with photolysis-resistant compounds and depleted in photoreactive compounds. This was further verified by comparing the isomer ratios of B*a*A/Chr and B*a*P/P*e*P in the spring samples (0.1−0.2 and 0.0−0.1) with those in the summer samples (0.3−0.4 and 0.6−0.8). Therefore, aerosols collected in spring may have been subject to longer-range atmospheric transport than those collected in summer.

Assessment of PAH Input Pathways. The results presented above classified the PAH compounds into two to five clusters (or principal components) for all the samples. Particularly, PC1 and PC2 for sediments, street dusts, and aerosols from Macao and Nanhai were mainly comprised of alkylated and S/O PAHs (petrogenic) and high-molecular-weight parent PAHs (pyrogenic), respectively. Furthermore, a score plot of PC1 and PC2 for all the samples (Figure 5) shows that all sediments except for those from Port Interior and aerosols of nonpoint sources from Macao and Nanhai are clustered in one group near the origin. We therefore propose that atmospheric deposition, direct (i.e., dry and wet deposition in coastal areas) or indirect (i.e., deposition to the Delta's watershed and transport to the coastal areas via surface runoff), would be the dominant pathway for most PAHs (e.g., alkylated, S/O, and HMW-PAHs) to reach the coastal sediments of Macao. Further assessments to validate this notion are given below.

Since benzo[*a*]anthracene and benzo[*a*]pyrene are photodegraded more easily than their isomers, chrysene and benzo-[*e*]pyrene, respectively, during transportation (*68*), the ratios of B*a*A/Chr and B*a*P/B*e*P can be used as tracers for the degree of photodegradation in addition to being used as source discriminators. Figure 6 shows a plot of B*a*A/Chr versus B*a*P/B*e*P for all the samples, and several features can be observed. First, the correlation between B*a*A/Chr and B*a*P/B*e*P was poor ($r^2 = 0.25$) in the sediment samples, implying two possible discrete sources or transport modes for the isomer

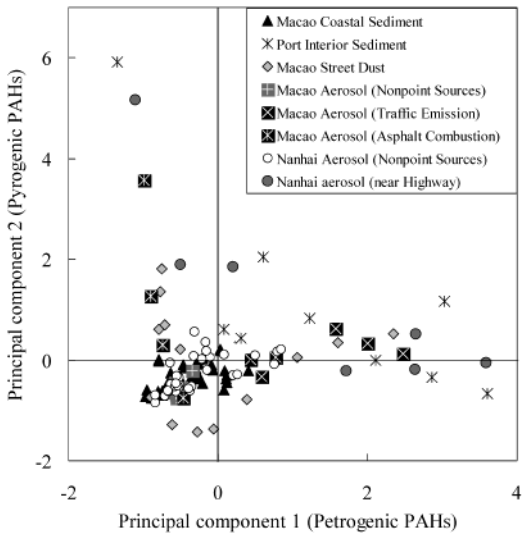

FIGURE 5. Comparison of principal components, PC1 (petrogenic) and PC2 (pyrogenic), for sediment, aerosol, and street dust samples collected from the coast of Macao and the Pearl River Delta.

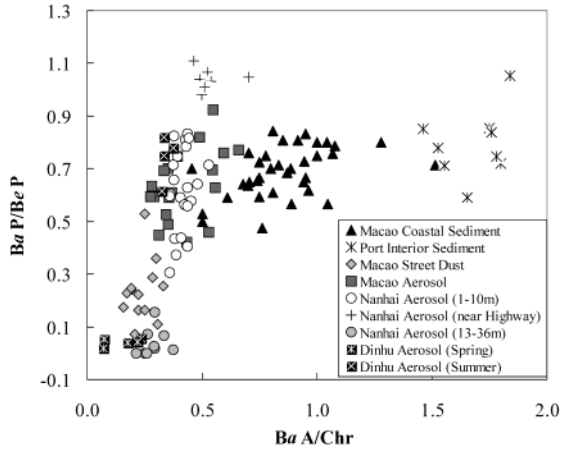

FIGURE 6. Compositional relationships between benzo[*a*]anthracene/chrysene (B*a*A/Chr) and benzo[*a*]pyrene/benzo[*e*]pyrene (B*a*P/B*e*P) determined in sediments, street dusts, and aerosols from Macao and aerosols from Nanhai and Dinhu Mountain.

pairs. Second, B*a*A/Chr values for Port Interior sediments (1.5−1.8) were higher than those for other sediments (0.5−1.5), aerosols (0.1−0.7), and street dusts (0.2−0.3). On the other hand, B*a*P/B*e*P varied only slightly with sediments collected at different locations (0.5−1.1), and the sediment values were similar to those in aerosol samples (0.4−0.9) from Macao and Nanhai (at altitudes of 1−10 m) but higher than those in street dusts (0.07−0.5) and lower than those in aerosols collected near a highway of Nanhai (0.98−1.11). It appeared that aerial deposition was a major route for high-molecular-weight PAH compounds to reach sediments, and Port Interior might be closer to the potential sources of benzo[*a*]anthracene and chrysene than other waterways. Third, aerosols collected from Nanhai at high altitudes (13−36 m) and Dinhu Mountain during spring season had the lowest values of B*a*A/Chr and B*e*P/B*a*P among all the samples. This may have resulted from high degree of photodegradation during atmospheric transport, and therefore the high-molecular-weight PAHs may have been transported from outside the Pearl River Delta.

Additional assessments (Supporting Information) indicated that high-molecular-weight PAHs in Macao's coastal sediments were imported mainly via dry and wet deposition of atmospheric particles. In additions, both atmosphere deposition and street runoff could be significant input pathways for alkylated and S/O PAHs found in the coast of Macao. Also in summer time, aerosols collected on Dinhu Mountain, a relatively less urbanized area, appeared to be predominantly derived from other highly industrialized and urbanized regions around the Pearl River Delta and could deposit in the Xijiang River watershed and subsequently transported into the coastal waters off Macao and the Pearl River Estuary by river runoff.

Acknowledgments

This research was financially supported by the Natural Science Foundation of the People's Republic of China (Project Nos. 40272129 and 49972094), the Chinese Academy of Sciences (No. ZKCX2-SW-212), and the Guangdong Natural Science Foundation (No. 010504). The authors thank Professor Y. S. Min for his help in collecting sediment samples and Ms. Z. Lin for her assistance in GC/MS analysis. The anonymous reviewers are also sincerely appreciated for their critical reviews that greatly improved this paper.

Supporting Information Available

An assessment of transport pathways of PAHs, tables outlining the sample characteristics and concentrations of individual PAHs in all the samples, and figures presenting the relationships between total PAHs (tPAH1) and BC, OC, and clay contents, PAH profiles, PCA results, and triangular diagrams illustrating the relative abundances of various parent, alkylated, and S/O PAHs in sediment, street dust, and aerosol samples. This material is available free of charge via the Internet at http://pubs.acs.org.

Literature Cited

(1) Tanabe, S. *Mar. Pollut. Bull.* **1991**, *22*, 259−260.
(2) Iwata, H.; Tanabe, S.; Sakai, N.; Nichimura, A.; Tatsukawa, R. *Environ. Pollut.* **1994**, *85*, 15−33.
(3) Zakaria, M. P.; Takada, H.; Tsutsumi, S.; Ohno, K.; Yamada, J.; Kouno, E.; Kumata, H. *Environ. Sci. Technol.* **2002**, *36*, 1907−1918.
(4) Zhang, G.; Parker, A.; House, A.; Mai, B.; Kang, Y.; Wang, Z. *Environ. Sci. Technol.* **2002**, *36*, 3671−3677.
(5) Wania, F.; Mackay, D. *Environ. Sci. Technol.* **1996**, *30*, 390A−396A.
(6) Bignert, A.; Olsson, M.; Persson, W.; Jensen, S.; Zakrisson, S.; Litzen, K.; Eriksson, U.; Haggberg, L.; Alsberg, T. *Environ. Pollut.* **1998**, *99*, 177−198.
(7) Simonich, S. L.; Hites, R. A. *Science* **1995**, *269*, 1851−1854.
(8) Iwata, H.; Tanabe, S.; Sakai, N.; Tatsukawa, R. *Environ. Sci. Technol.* **1993**, *27*, 1080−1098.
(9) Hong, H.; Xu, L.; Zhang, L.; Chen, J. C.; Wong, Y. S.; Wan, T. S. M. *Mar. Pollut. Bull.* **1995**, *31*, 229−236.
(10) Zhou, J. L.; Hong, H.; Zhang, Z.; Maskaoui, K.; Chen, W. *Water Res.* **2000**, *34*, 2132−2150.
(11) Yang, G.-P. *Environ. Pollut.* **2000**, *108*, 163−171.
(12) Hong, H. S.; Wang, X. H.; Xu, L.; Chen, W. Q.; Zhang, L. P.; Zhang, Z. L. *J. Environ. Sci. Heal. A* **2000**, *35*, 1833−1847.
(13) Mai, B. X.; Sheng, G. Y.; Lin, Z.; Zhang, G.; Min, Y. S.; Fu, J. M. *Chin. Sci. Bull.* **2000**, *45*, 97−104 Suppl. S.
(14) Yuan, D. X.; Yang, D. N.; Wade, T. L.; Qian, Y. R. *Environ. Pollut.* **2001**, *114*, 101−111.
(15) Tam, N. F. Y.; Ke, L.; Wang, X. H.; Wong, Y. S. *Environ. Pollut.* **2001**, *114*, 255−263.
(16) Mai, B.; Fu, J.; Zhang, G.; Lin, Z.; Min, Y.; Sheng, G.; Wang, X. *Appl. Geochem.* **2001**, *16*, 1429−1445.
(17) Maskaoui, K.; Zhou, J. L.; Hong, H. S.; Zhang, Z. L. *Environ. Pollut.* **2002**, *118*, 109−122.
(18) Mai, B.; Fu, J.; Sheng, G.; Kang, Y.; Lin, Z.; Zhang, G.; Min, Y.; Zeng, E. Y. *Environ. Pollut.* **2002**, *117*, 457−474.
(19) Guangzhou Planning Association and Guangzhou Territory Planning Association. In *The Territory Resources of Guangzhou*; Guangzhou, P. R., Ed.; Guangzhou Press: China, 1994; pp 47−67 (in Chinese).
(20) Kang, Y.; Sheng, G.; Fu, J.; Mai, B.; Zhang, G.; Lin, Z.; Min, Y. *Mar. Pollut. Bull.* **2000**, *40*, 794−797.

(21) Luo, X.; Yang, Q.; Jia, L. *River-Bed Evolution of the Pearl River Delta*; Guangzhou, P. R., Ed.; Zhongshan University Press: China, 2002 (in Chinese).
(22) Qi, S.; Yan, J.; Zhang, G.; Fu, J.; Sheng, G.; Wang, Z.; Tang, S.; Deng, Y.; Min, Y. *Environ. Monitor. Assess.* **2001**, *72*, 115−127.
(23) Gustafsson, Ö.; Haghseta, F.; Chan, C.; MacFarlane, J.; Gschwend, P. M. *Environ. Sci. Technol.* **1997**, *31*, 203−209.
(24) Meglan, R. R. *Mar. Chem.* **1992**, *39*, 217−237.
(25) Harrison, R. M.; Smith, D. J. T.; Luhana, L. *Environ. Sci. Technol.* **1996**, *30*, 825−832.
(26) Kavouras, I. G.; Koutrakis, P.; Tsapakis, M.; Lagoudaki, E.; Stephanou, E. G.; Baer, D. V.; Oyola, P. *Environ. Sci. Technol.* **2001**, *35*, 2288−2294.
(27) Hites, R. A.; LaFlamme, R. E.; Windsor, J. G., Jr. *Geochim. Cosmochim. Acta* **1980**, *44*, 873−878.
(28) Wakeham, S. G.; Schaffner, C.; Giger, W. *Geochim. Cosmochim. Acta* **1980**, *44*, 415−429.
(29) Tan, Y. L.; Heit, M. *Geochim. Cosmochim. Acta* **1981**, *45*, 2267−2279.
(30) Renberg, I.; Persson, M. W.; Emteryd, O. *Nature* **1994**, *368*, 323−326.
(31) Wakeham, S. G.; Schaffner, C.; Giger, W.; Boon, J. J.; Leeuw, J. W. D. *Geochim. Cosmochim. Acta* **1979**, *43*, 1141−1144.
(32) Venkatesan, M. I. *Mar. Chem.* **1988**, *25*, 1−27.
(33) Tolosa, J.; Bayona, J. M.; Albaigés, J. *Environ. Sci. Technol.* **1996**, *30*, 2495−2503.
(34) Canton, L.; Grimalt, J. O. *J. Chromatogr.* **1992**, *607*, 279−286.
(35) Ramdahl, T. *Nature* **1983**, *306*, 580−582.
(36) MaGroddy, S. E.; Farrington, J. W. *Environ. Sci. Technol.* **1995**, *29*, 1542−1550.
(37) Maruya, K. A.; Risebrough, R. W.; Horne, A. J. *Environ. Sci. Technol.* **1996**, *30*, 2942−2947.
(38) Luthy, R. G.; Alken, G. R.; Brusseau, M. L.; Cunningham, S. D.; Gschwend, P. M.; Pignatello, J. J.; Reinhard, M.; Traina, S. J.; Weber, W. J., Jr.; Westall, J. C. *Environ. Sci. Technol.* **1997**, *31*, 3341−3347.
(39) Næs, K.; Axelman, J.; Näf, C.; Broman, D. *Environ. Sci. Technol.* **1998**, *32*, 1786−1792.
(40) Lamoureux, E. M.; Brownawell, B. J. *Environ. Toxicol. Chem.* **1999**, *18*, 1733−1741.
(41) Ghosh, U.; Gillette, J. S.; Luthy, R. G.; Zare, R. N. *Environ. Sci. Technol.* **2000**, *34*, 1729−2736.
(42) Accardi-Dey, A.; Gschwend, P. M. *Environ. Sci. Technol.* **2002**, *36*, 21−29.
(43) Gustafsson, Ö.; Gschwend, P. M. In *Molecular Markers in Environmental Geochemistry;* ACS Symposiun Series 671; Eganhouse, R. P., Ed.; American Chemical Society: Washington, DC, 1997; pp 365−381.
(44) Gustafsson, Ö.; Gschwend, P. M. *Geochim. Cosmochim. Acta* **1998**, *62*, 465−472.
(45) Karickhoff, S. W.; Brown, D. S.; Scott, T. A. *Water Res.* **1979**, *13*, 241−248.
(46) Chiou, C. T.; Peters, J.; Freed, V. H. *Science* **1979**, *206*, 831−832.
(47) Arzayus, K. M.; Dickhut, R. M.; Canuel, E. A. *Environ. Sci. Technol.* **2001**, *35*, 2178−2180.
(48) Laflamme, R. E.; Hites, R. A. *Geochim. Cosmochim. Acta* **1978**, *42*, 289−303.
(49) Lake, J. L.; Norwood, C.; Dimock, C.; Bowen, R. *Geochim. Cosmochim. Acta* **1979**, *43*, 1847−1854.
(50) Yunker, M. B.; Snowdon, L. R.; Macdonald, R. W.; Smith, J. N.; Fowler, M. G.; Skibo, D. N.; Mclaughlin, F. A.; Danyushevskaya, A. I.; Petrova, V. I.; Ivanov, G. I. *Environ. Sci. Technol.* **1996**, *30*, 1310−1320.
(51) Lee, M. L.; Prado, G. P.; Howard, J. B.; Hites, R. A. *Biomed. Mass Spectrom.* **1977**, *4*, 182−186.
(52) Youngblood, W. W.; Blumer, M. *Geochim. Cosmochim. Acta* **1975**, *39*, 1303−1313.
(53) Garrigues, P.; Budzinski, H.; Manitz, M. P.; Wise, S. A. *Polycycl. Aromat. Comput.* **1995**, *7*, 275−284.
(54) Takada, H.; Onda, T.; Harada, M.; Ogura, N. *Sci. Total Environ.* **1991**, *107*, 45−69.
(55) Maher, W. A.; Aislabie, J. *Sci. Total Environ.* **1992**, *112*, 143−164.
(56) Marvin, C. H.; McCarry, B. E.; Villella, J.; Allan, L. M.; Bryant, D. W. *Chemosphere* **2000**, *41*, 979−988.
(57) Dickhut, R. M.; Canuel, E. A.; Gustafson, K. E.; Liu, K.; Arzayus, K. M.; Walker, S. E.; Edgecombe, G.; Gaylor, M. O.; MacDonald, E. H. *Environ. Sci. Technol.* **2000**, *34*, 4635−4640.
(58) Bjorseth, A.; Ramdahl, T. In *Handbook of Polycyclic Aromatic Hydrocarbons*; Bjorseth, A., Ramdahl, T., Eds.; Marcel Dekker: New York, 1985; Vol. 2, Chapter 1.
(59) Mitra, S.; Bianchi, T. S.; McKee, B. A.; Sutula, M. *Environ. Sci. Technol.* **2002**, *36*, 2296−2302.
(60) Colmsjö, A. L.; Zebühr, Y. U.; Östman, C. E. *Chemosphere* **1986**, *15*, 169−182.
(61) Gustafson, K. E.; Dickhut, R. M. *Environ. Sci. Technol.* **1997**, *31*, 1623−1629.
(62) Tsai, P.; Hoenicke, R.; Yee, D. *Environ. Sci. Technol.* **2002**, *36*, 4741−4747.
(63) Hoff, R. M.; Strachan, W. M. J.; Sweet, C. W.; Chan, C. H.; Shackleton, M.; Bidleman, T. F.; Brice, K. A.; Burniston, D. A.; Cussion, S.; Gatz, D. F.; Harlin, K.; Schroeder, W. H. *Atmos. Environ.* **1996**, *30*, 3505−3527.
(64) Eisenreich, S. J.; Hornbuckle, K. C.; Achman, D. R. In *Atmospheric Deposition of Contaminants to the Great Lakes and Costal Water*; Baker, J. E., Ed.; SETAC: Pensacola, FL, 1997; pp 109−136.
(65) Gigliotti, C. L.; Brunciak, P. A.; Dachs, J.; Glenn, T. R., IV.; Nelson, E. D.; Totten, L. A.; Eisenreich, S. J. *Environ. Toxicol. Chem.* **2002**, *21*, 235−244.
(66) Simcik, M. F.; Eisenreich, S. J.; Lioy, P. J. *Atmos. Environ.* **1999**, *33*, 5071−5079.
(67) Sporstøl, S.; Gjøs, N.; Lichtenthaler, R. G.; Gustavsen, K. O.; Urdal, K.; Oreld, F.; Skel, J. *Environ. Sci. Technol.* **1983**, *17*, 282−286.
(68) Butler, J. D.; Crossley, P. *Atmos. Environ.* **1981**, *15*, 91−94.

Received for review May 22, 2003. Revised manuscript received August 15, 2003. Accepted August 20, 2003.

ES034514K